Supporting Information

Synergistic Electronic Coupling/Cross-talk between the Isolated Metal Halide Units of Zero Dimensional Heterometallic (Sb, Mn) Halide Hybrid with Enhanced Emission

Anupam Biswas,[1,2] Rangarajan Bakthavatsalam,[3] Deep K. Das,[3] Jisvin Sam,[3] Bhupendra P. Mali,[1,2] Chinmoy Biswas,[4] Narugopal Maana,[1,2] Stuart Thomson,[5] Sai Santosh Kumar Raavi,[4] Sreekumar Kurungot,[1,2] Rajesh G Gonnade,[1,2] Sudipta Dutta,[3] Janardan Kundu*[,4]

[1]CSIR-National Chemical Laboratory, Pune, India.

[2]Academy of Scientific and Innovative Research (AcSIR), Ghaziabad, India.

[3]Indian Institute of Science Education and Research (IISER) Tirupati, Tirupati, India

[4]Indian Institute of Technology Hyderabad, Kandi, India.

[5]Edinburgh Instruments Ltd, Kirkton Campus, EH54 7DQ, United Kingdom.

Conductivity measurement:

Powders of Tris SbMnCl hybrid was pressed for 2 minutes under 1000 psi to obtain uniform thickness pellets (~1.1 mm in thickness, 13 mm in diameter). The proton conductivity was measured at a range of temperatures (from 30 ^{o}C to 50 ^{o}C) under 80% RH. Pouillet's equation, $\sigma = L/(R \times A)$ was employed to calculate the proton conductivity, wherein σ is the conductivity (S cm^{-1}), L is the thickness of the measured sample (cm), and A is the electrode area (in cm^2). The resistance is calculated using the high-frequency intercept of the Nyquist plot measured by the impedance spectroscopy. To determine the activation energy corresponding to proton conduction at different temperatures:

$$\sigma = \sigma_o e^{\left(\frac{-E_a}{kT}\right)}$$

where σ and σ_o denote conductivity and pre-exponential factor, respectively, T indicates the absolute temperature in kelvin, E_a indicates the activation energy, and k denotes the Boltzmann constant.

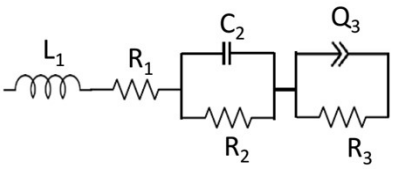

L1: Inductance
R1, **R2** & **R3**: Resistance
C2: Capacitance
Q3: Constant phase element

Equivalent Circuit: **L1+R1+C2/R2+Q3/R3**

An equivalent circuit shown above is used to fit the data.[1]

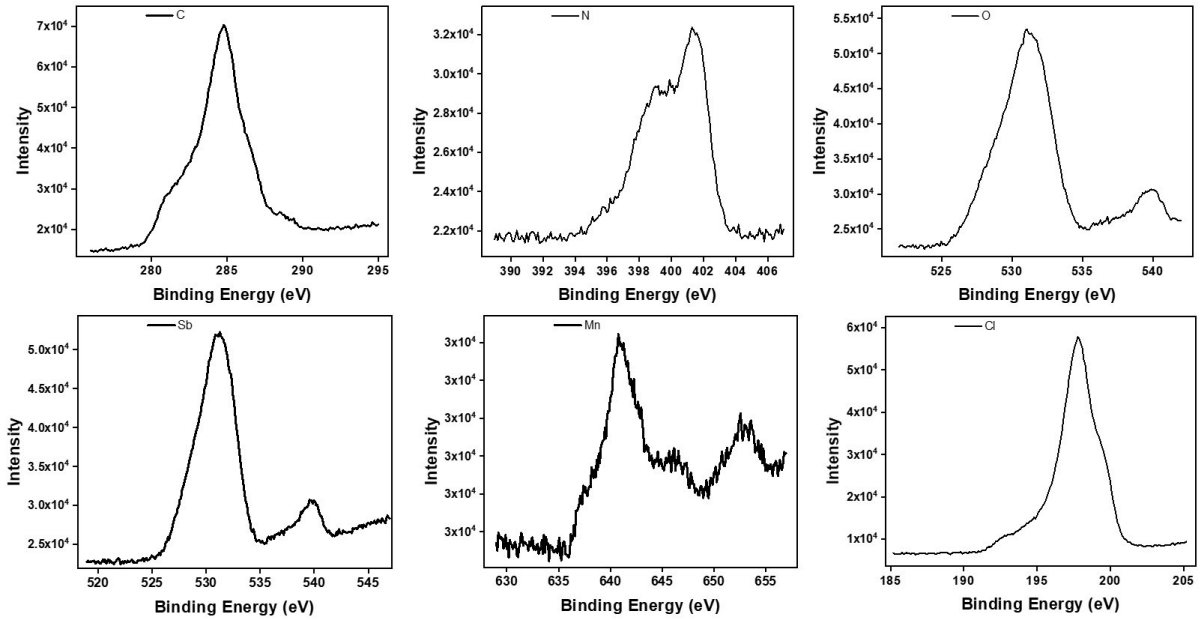

Figure S1: XPS analysis of Tris SbMnCl hybrid

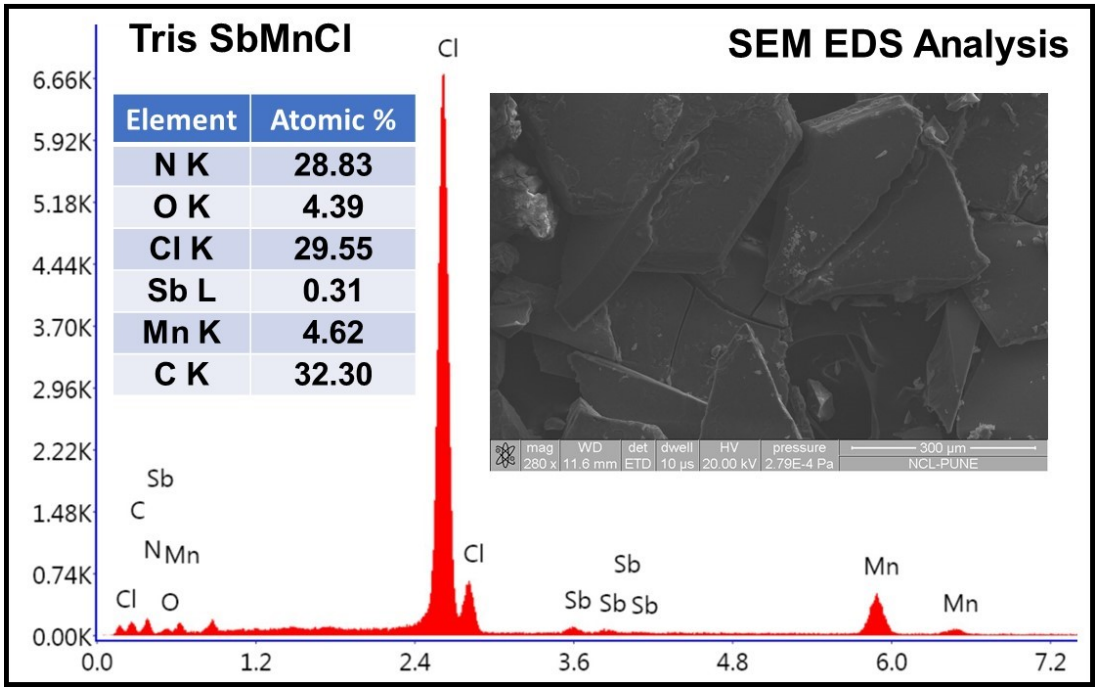

Figure S2: SEM-EDS analysis of Tris SbMnCl hybrid

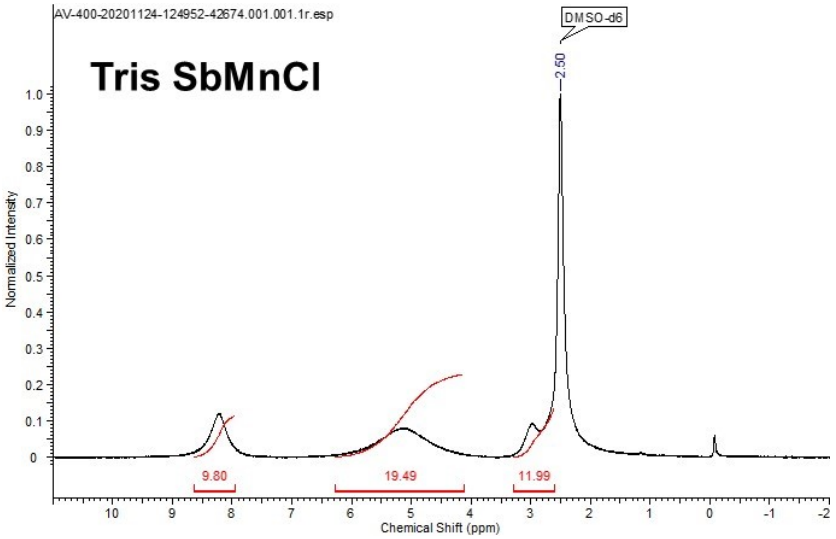

Figure S3: ^{1}H NMR of Tris SbMnCl (400 MHz, DMSO-d6, 298 K): δ 8.2 (br, 9H, NH3), 3.02 (br, 12H, CH2), 5.1 (br, 18H, H2O & 1H, NH) ppm.

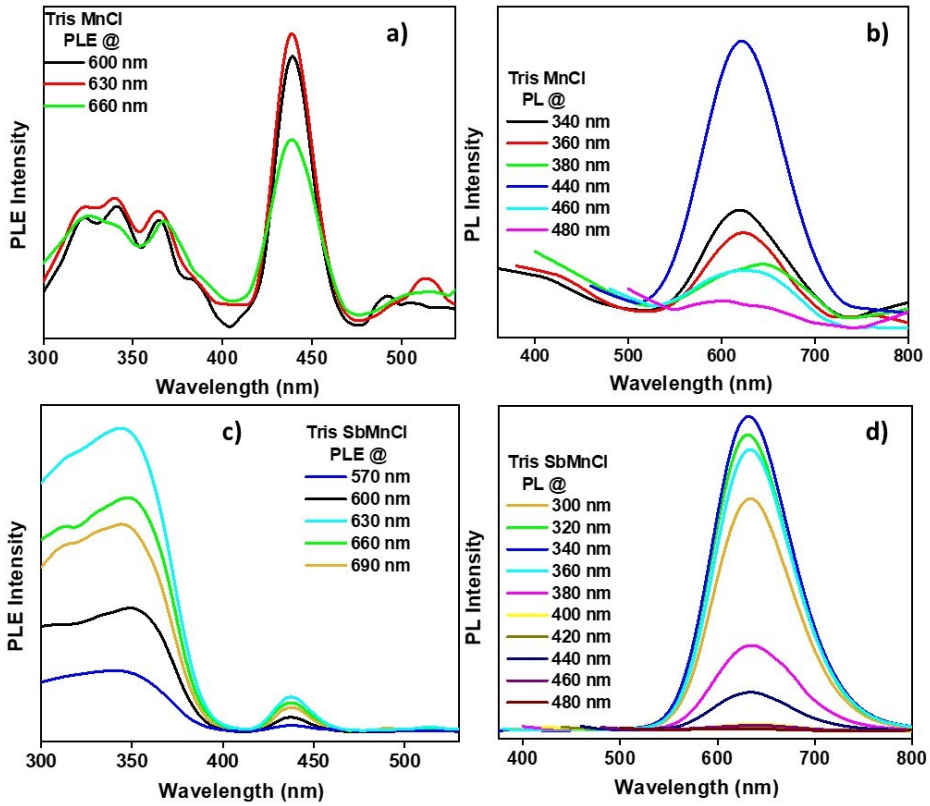

Figure S4: PLE collected across the emission band (a,c) and excitation dependent PL (b,d) for Tris MnCl and Tris SbMnCl hybrid.

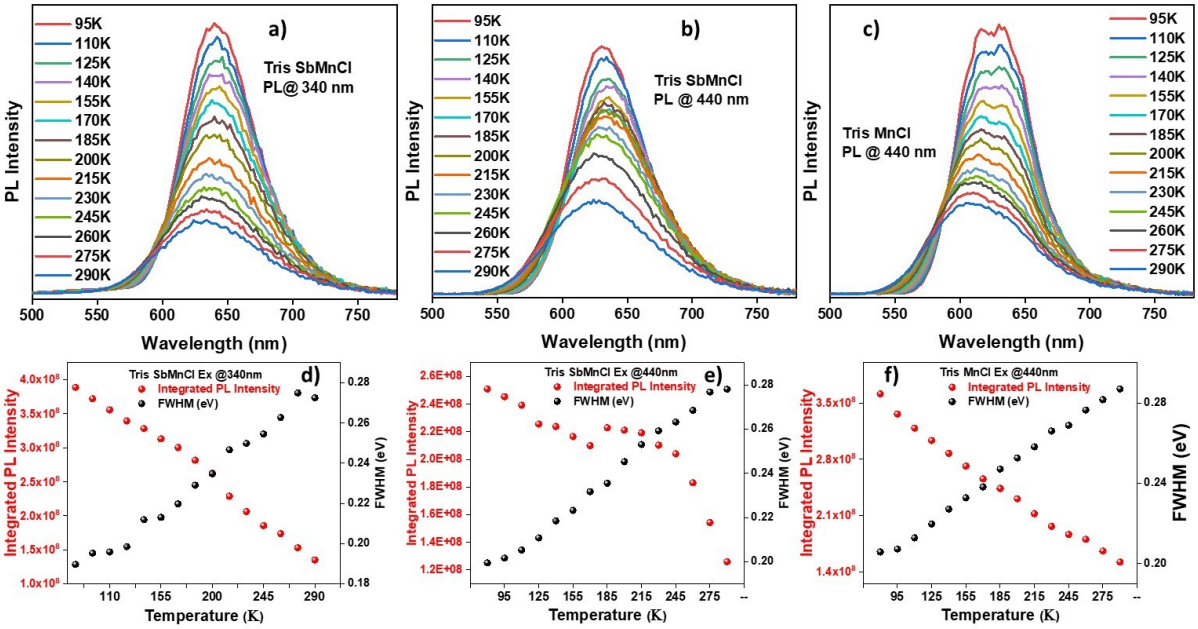

Figure S5: Comparison of the evolution of low temperature PL profile of Tris SbMnCl excited at a) 340 nm, b) 440 nm and Tris MnCl hybrid excited at c) 440 nm; Comparison of the evolution of integrated PL intensity and bandwidth of Tris SbMnCl excited at d) 340 nm, e) 440 nm and Tris MnCl hybrid excited at f) 440 nm across the temperature range investigated.

Table S1: Temperature dependent lifetime values and their relative contributions for Tris SbMnCl hybrid excited at 340 nm over millisecond timescales

Temperature (K)	Lifetime (ms)	Relative %
110	3	20.1
	13	79.9
155	2.9	22.2
	12.2	77.8
200	2.8	27.0
	11.4	73.0
245	2.5	34.8
	10.3	65.2
290	2.2	38.3
	8.7	61.7

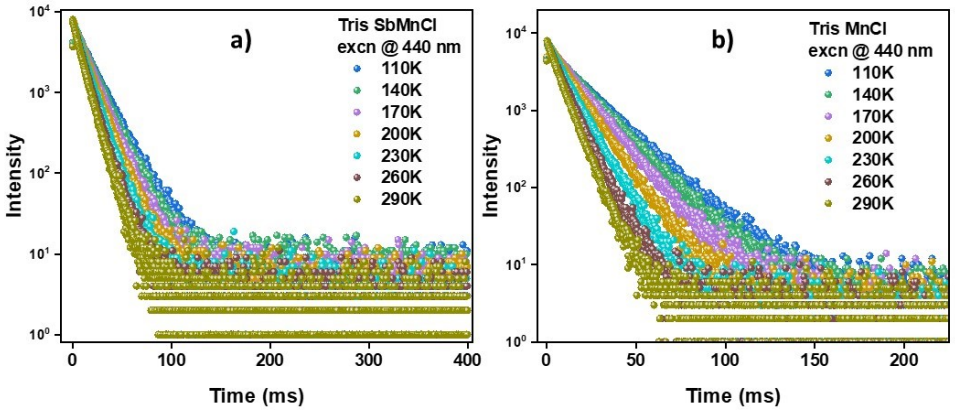

Figure S6: Temperature dependent lifetime PL decay profiles excited at 440 nm of a) Tris SbMnCl and b) Tris MnCl collected over millisecond timescales.

Table S2: Temperature dependent lifetime values and their relative contributions for Tris SbMnCl and Tris MnCl hybrid excited at 440 nm over millisecond timescales.

Tris SbMnCl			Tris MnCl		
Temp.	Lifetime (ms)	Relative %	Temp.	Lifetime (ms)	Relative %
290K	6.3	34.84	290K	5.8	62.56
	10.7	65.16		9.1	37.44
260K	8.2	52.85	260K	6.8	43.44
	12.6	47.15		9.7	56.56
230K	10.4	81.1	230K	7.1	26.41
	15.8	18.9		11.2	73.59
200K	10.5	44.52	200K	7.6	13.17
	14.7	55.48		13.1	86.83
170K	5.26	3.25	170K	10.2	18.51
	14.6	96.75		16.1	81.49
140K	4.1	2.87	140K	0.5	0.91
	16.1	97.13		17.6	99.09
110K	6.5	8.87	110K	2.2	2.39
	18.3	91.33		19.8	97.61

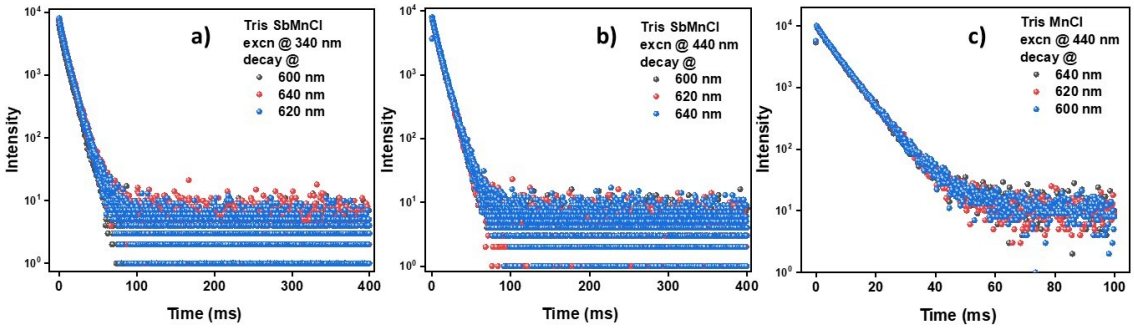

Figure S7: Room temperature PL decay profiles collected over millisecond timescales across the emission band of Tris SbMnCl excited at a) 340 nm, b) 440 nm; and of Tris MnCl excited at c) 440 nm.

Table S3: Room temperature lifetime values and their relative contributions for Tris SbMnCl hybrid excited at 340 nm over millisecond timescales across the emission band.

Ex 340 Emission wavelength	Tris SbMnCl Lifetime (ms)	Relative %
600nm	4.1	20.2
	9.8	79.8
620nm	4.8	27.1
	10.1	62.9
640nm	4.9	28.5
	10.3	71.5

Table S4: Room temperature lifetime values and their relative contributions for Tris SbMnCl hybrid excited at 440 nm over millisecond timescales across the emission band.

Ex 440 Emission wavelength	Tris SbMnCl Lifetime (ms)	Relative %
600nm	6.3	38.9
	10.6	61.1
620nm	6.1	37.3
	10.6	62.7
640nm	7	56.5
	11.7	43.5

Table S5: Room temperature lifetime values and their relative contributions for Tris MnCl hybrid excited at 440 nm over millisecond timescales across the emission band.

Ex 440 Emission wavelength	Tris MnCl Lifetime (ms)	Relative %
600nm	4.6	25.9
	7.4	74.1
620nm	3.9	16.1
	7.2	83.9
640nm	3.6	12.6
	7.1	87.4

Table S6: Temperature dependent lifetime values and their relative contributions for Tris SbMnCl hybrid excited at 340 nm over microsecond timescales.

Temperature (K)	Lifetime (µs)	Relative %
110	0.2	1.4
	3.5	98.6
155	0.3	2.1
	3.2	97.9
200	0.3	4.1
	3.1	95.9
245	0.6	10.7
	2.9	89.3
290	0.3	33.6
	1.3	66.4

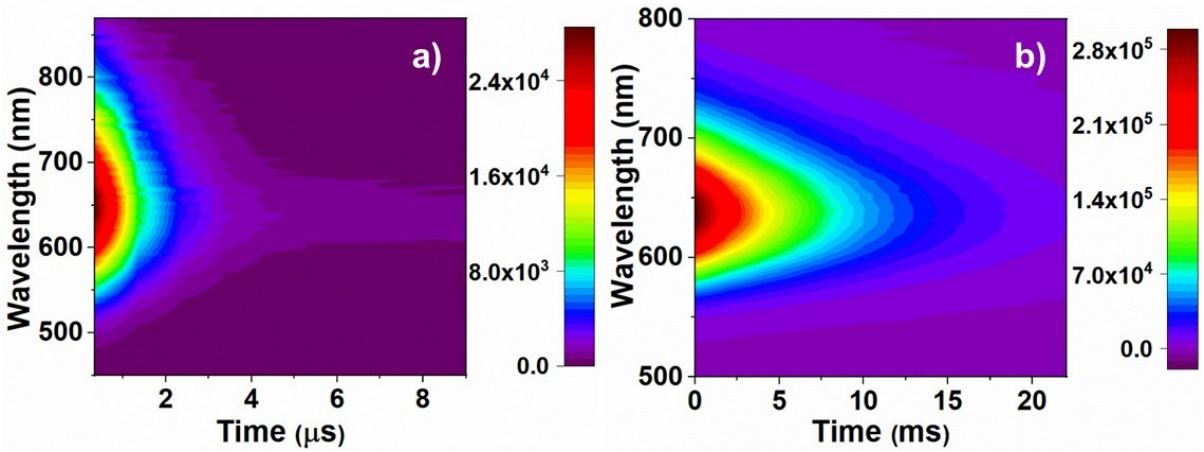

Figure S8: Contour plot of time resolved emission spectra (**TRES**) of Tris SbMnCl hybrid excited at 340 nm collected over a) microsecond and b) millisecond timescales.

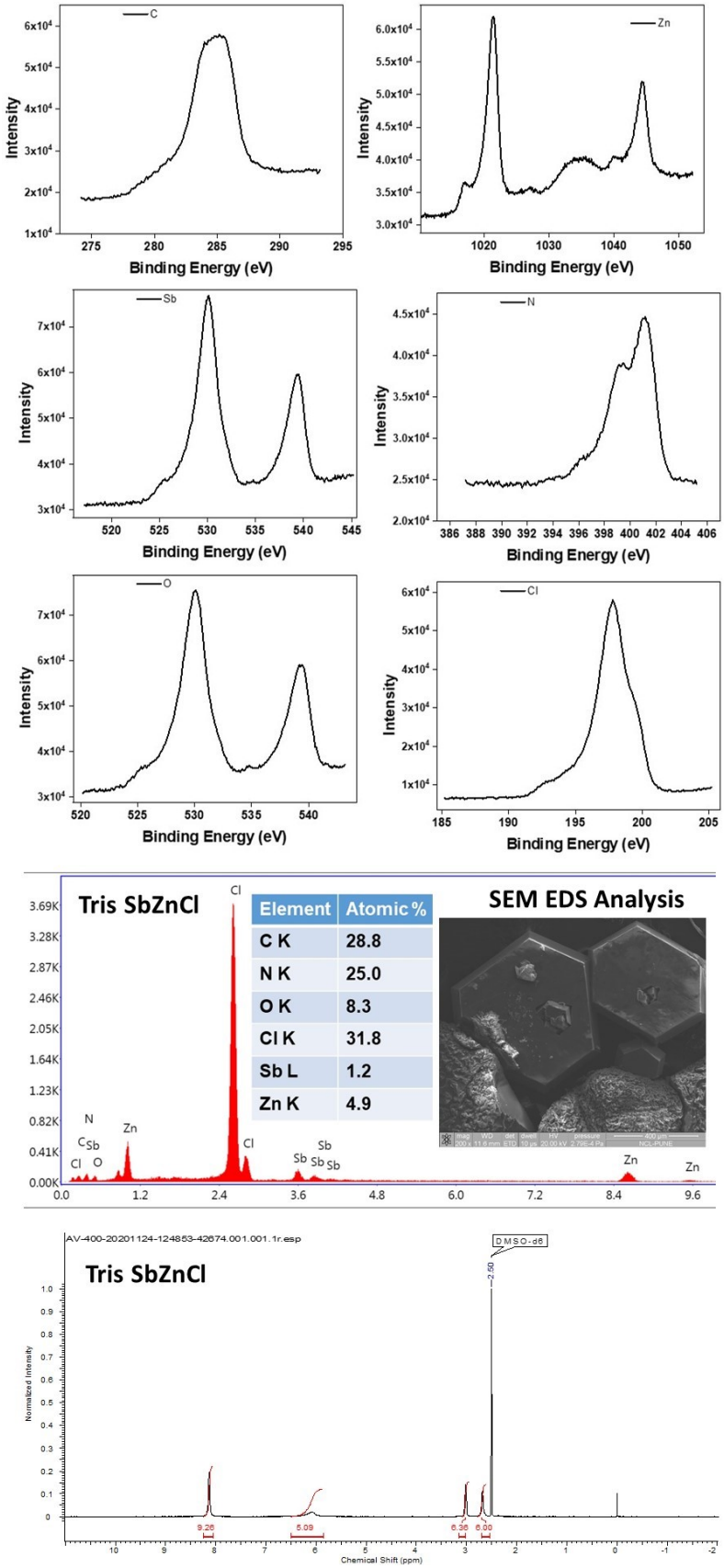

Figure S9: Tris SbZnCl hybrid- XPS, SEM-EDS, and ^{1}H NMR (400 MHz, DMSO-d6, 298 K) analysis: δ 8.2 (br, 9H, NH_3), 3.02 (br, 6H, CH_2), 2.70 (br, 6H, CH_2), 6.1 (br, 4H, H_2O & 1H, NH) ppm.

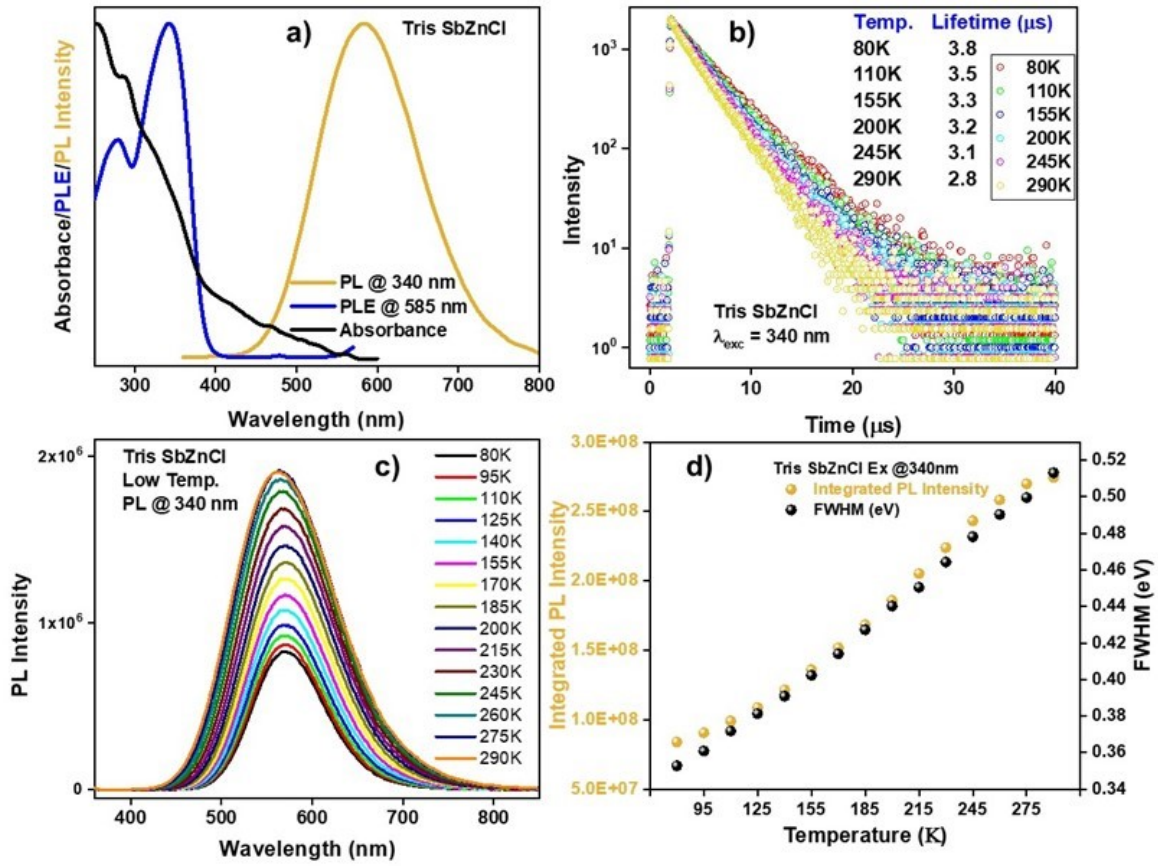

Figure S10: Optical characterization of Tris SbZnCl hybrid excited at 340 nm showing a) Absorbance, PL, PLE; b) lifetime decay profiles collected at emission maxima across temperature range investigated along with the fitted lifetime values in microseconds; evolution of c) PL profile and d) integrated PL intensity and bandwidth across temperature range investigated.

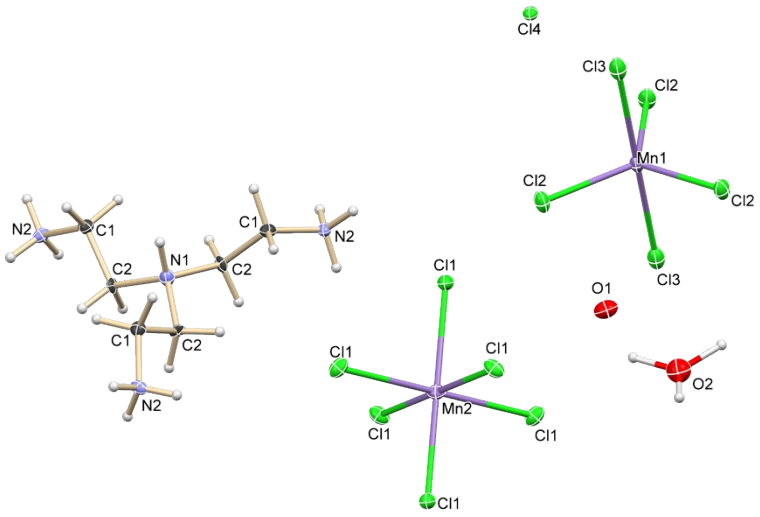

Figure S11: ORTEP view of the asymmetric unit of Tris MnCl hybrid showing the atom-numbering scheme. The displacement ellipsoids are drawn at the 50% probability level and H atoms are shown as small spheres with arbitrary radii.

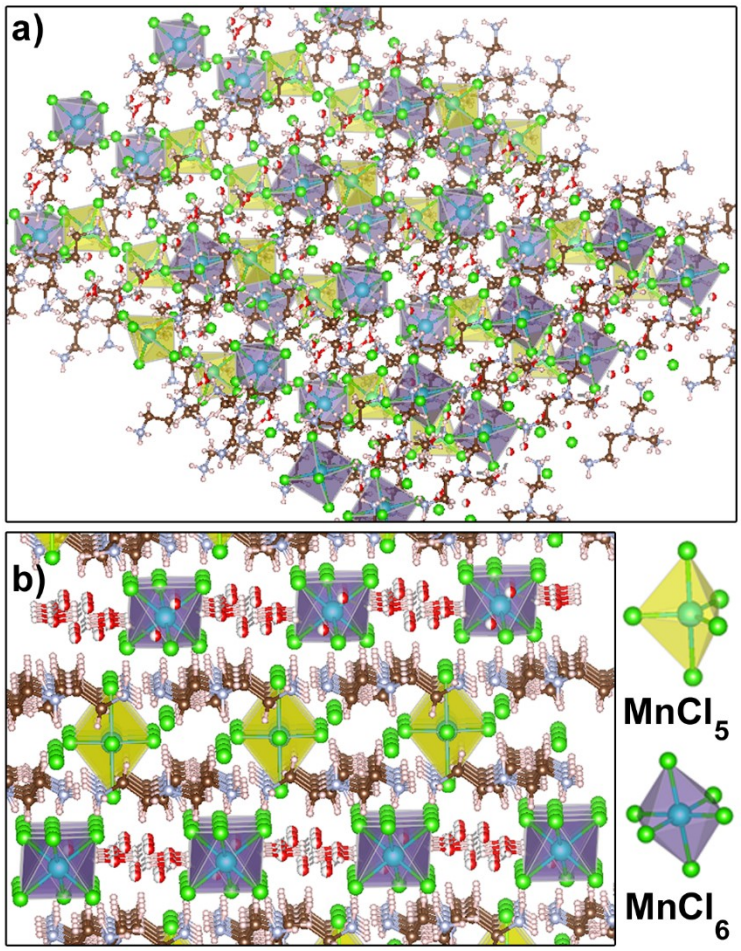

Figure S12: SCXRD structure of Tris MnCl hybrid highlighting a) 0D metal halide units (isolated $MnCl_5$, isolated $MnCl_6$ units) surrounded by organic ligands and b) plane containing the isolated $MnCl_6$ units have water molecules while tbp plane is devoid of water molecules.

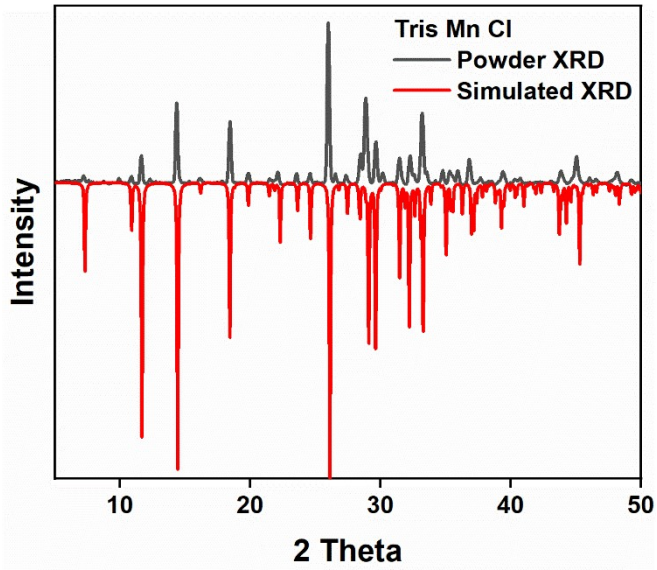

Figure S13: Comparison of the experimental and simulated PXRD patterns for Tris MnCl hybrid showing good match.

Table S7. Sample and crystal data for Tris MnCl.

Identification code	Mn_Tris_Cl	
Chemical formula	$C_{12}H_{47}Cl_{13}Mn_2N_8O_4$	
Formula weight	938.30 g/mol	
Temperature	100(2) K	
Wavelength	0.71073 Å	
Crystal size	0.090 × 0.160 × 0.220 mm	
Crystal system	trigonal	
Space group	*R*-3*c*	
Unit cell dimensions	a = 9.6122(5) Å	α = 90°
	b = 9.6122(5) Å	β = 90°
	c = 72.494(5) Å	γ = 120°
Volume	5800.7(7) Å^3	
Z	6	
Density (calculated)	1.612 g/cm^3	
Absorption coefficient	1.583 mm^{-1}	
F(000)	2868	

Table S8. Data collection and structure refinement for Tris MnCl.

Theta range for data collection	2.69 to 26.00°
Index ranges	-11<=h<=11, -11<=k<=11, -89<=l<=89
Reflections collected	28639
Independent reflections	1279 [R(int) = 0.0840]
Coverage of independent reflections	99.6%
Absorption correction	Multi-Scan
Max. and min. transmission	0.8710 and 0.7220
Structure solution technique	direct methods
Structure solution program	SHELXT 2014/5 (Sheldrick, 2014)
Refinement method	Full-matrix least-squares on F^2
Refinement program	SHELXL-2018/3 (Sheldrick, 2018)
Function minimized	$\Sigma\, w(F_o^2 - F_c^2)^2$
Data / restraints / parameters	1279 / 13 / 68
Goodness-of-fit on F^2	1.418

Δ/σ_{max}	0.001	
Final R indices	1232 data; I>2σ(I)	R1 = 0.0897, wR2 = 0.2121
	all data	R1 = 0.0920, wR2 = 0.2133
Weighting scheme	w=1/[$\sigma^2(F_o^2)$+430.5334P] where P=(F_o^2+2F_c^2)/3	
Largest diff. peak and hole	1.686 and -1.608 eÅ^{-3}	
R.M.S. deviation from mean	0.198 eÅ^{-3}	

Table S9. Bond lengths (Å) for Tris MnCl.

Mn1-Cl2	2.371(3)	Mn1-Cl2#3	2.371(3)
Mn1-Cl2#4	2.371(3)	Mn1-Cl3	2.695(4)
Mn1-Cl3#1	2.695(4)	Cl1-Mn2	2.563(2)
N1-C2#5	1.509(9)	N1-C2#2	1.509(8)
N1-C2	1.510(9)	N1-H1	1.0
N2-C1	1.477(11)	N2-H2A	0.91
N2-H2B	0.91	N2-H2C	0.91
C1-C2	1.508(11)	C1-H1A	0.99
C1-H1AB	0.99	C2-H2AA	0.99
C2-H2AB	0.99	O2-H1W	1.163(3)

Symmetry transformations used to generate equivalent atoms:

#1	x-y+2/3, -y+4/3, -z+5/6
#2	-y+1, x-y-1, z
#3	-y+1, x-y+1, z
#4	-x+y, -x+1, z
#5	-x+y+2, -x+1, z

Table S10. Bond angles (°) for Tris MnCl.

Cl2-Mn1-Cl2#4	119.999(5)	Cl2-Mn1-Cl2#8	120.0010(10)
Cl2#4-Mn1-Cl2#8	120.0000(10)	Cl2-Mn1-Cl3	90.0
Cl2#4-Mn1-Cl3	90.0	Cl2#8-Mn1-Cl3	90.0
Cl2-Mn1-Cl3#1	90.0	Cl2#4-Mn1-Cl3#1	90.0
Cl2#8-Mn1-Cl3#1	90.0	Cl3-Mn1-Cl3#1	180.0
Cl1#5-Mn2-Cl1#6	89.60(7)	Cl1#5-Mn2-Cl1#7	89.60(7)
Cl1#6-Mn2-Cl1#7	89.60(7)	Cl1#5-Mn2-Cl1	180.0
Cl1#6-Mn2-Cl1	90.40(7)	Cl1#7-Mn2-Cl1	90.40(7)
Cl1#5-Mn2-Cl1#3	90.40(7)	Cl1#6-Mn2-Cl1#3	180.0
Cl1#7-Mn2-Cl1#3	90.40(7)	Cl1-Mn2-Cl1#3	89.59(7)
Cl1#5-Mn2-Cl1#9	90.40(7)	Cl1#6-Mn2-Cl1#9	90.40(7)
Cl1#7-Mn2-Cl1#9	180.0	Cl1-Mn2-Cl1#9	89.60(7)
Cl1#3-Mn2-Cl1#9	89.59(7)	C2#10-N1-C2#2	111.3(5)
C2#10-N1-C2	111.3(5)	C2#2-N1-C2	111.3(5)
C2#10-N1-H1	107.6	C2#2-N1-H1	107.6
C2-N1-H1	107.6	C1-N2-H2A	109.5
C1-N2-H2B	109.5	H2A-N2-H2B	109.5
C1-N2-H2C	109.5	H2A-N2-H2C	109.5
H2B-N2-H2C	109.5	N2-C1-C2	110.2(6)
N2-C1-H1A	109.6	C2-C1-H1A	109.6
N2-C1-H1AB	109.6	C2-C1-H1AB	109.6
H1A-C1-H1AB	108.1	C1-C2-N1	111.5(7)
C1-C2-H2AA	109.3	N1-C2-H2AA	109.3
C1-C2-H2AB	109.3	N1-C2-H2AB	109.3
H2AA-C2-H2AB	108.0		

Symmetry transformations used to generate equivalent atoms:

#1	x-y+2/3, -y+4/3, -z+5/6
#2	-y+1, x-y-1, z
#3	-y+1, x-y, z
#4	-y+1, x-y+1, z
#5	-x+4/3, -y+2/3, -z+2/3

#6	y+1/3, -x+y+2/3, -z+2/3
#7	x-y+1/3, x-1/3, -z+2/3
#8	-x+y, -x+1, z
#9	-x+y+1, -x+1, z
#10	-x+y+2, -x+1, z

Table S11. Torsion angles (°) for Tris MnCl.

N2-C1-C2-N1	167.4(7)	C2#2-N1-C2-C1	-80.4(12)
C2#1-N1-C2-C1	154.8(8)		

Symmetry transformations used to generate equivalent atoms:
#1 -y+1, x-y-1, z

#2 -x+y+2, -x+1, z

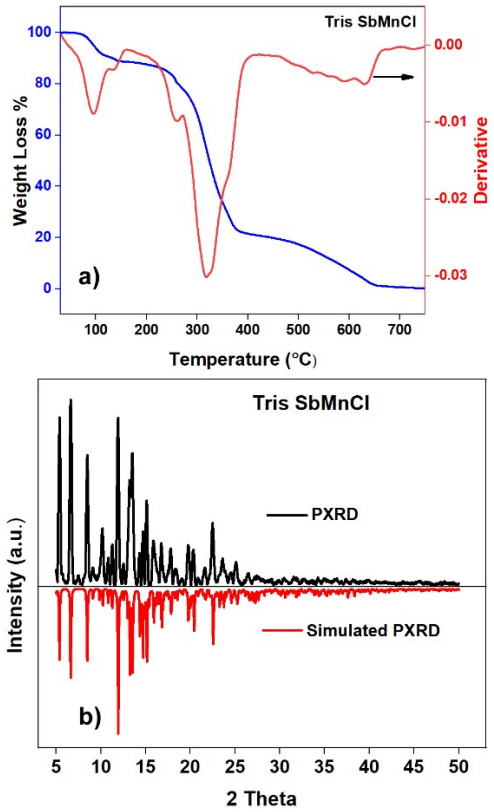

Figure S14. a) Thermogravimetric analysis of Tris SbMnCl hybrid showing water loss peak at ~ 100 °C; b) comparison of the experimental and simulated PXRD pattern of Tris SbMnCl hybrid.

Table S12. Sample and crystal data for Tris SbMnCl.

Identification code	SbMn_LowTemp_141220	
Chemical formula	$C_{12}H_{44}Cl_{13}Mn_{1.73}N_8O_6Sb_{0.27}$	
Formula weight	985.32 g/mol	
Temperature	100(2) K	
Wavelength	0.71073 Å	
Crystal size	0.090 x 0.120 x 0.230 mm	
Crystal system	trigonal	
Space group	R -3 c	
Unit cell dimensions	a = 9.5939(5) Å	α = 90°
	b = 9.5939(5) Å	β = 90°
	c = 72.574(5) Å	γ = 120°
Volume	5785.0(7) $Å^3$	
Z	6	
Density (calculated)	1.697 g/cm^3	
Absorption coefficient	1.695 mm^{-1}	
F(000)	2988	

Table S13. Data collection and structure refinement for Tris SbMnCl.

Theta range for data collection	2.52 to 25.99°	
Index ranges	-11<=h<=11, -11<=k<=11, -89<=l<=89	
Reflections collected	28391	
Independent reflections	1260 [R(int) = 0.0446]	
Max. and min. transmission	0.8620 and 0.6970	
Structure solution technique	direct methods	
Structure solution program	SHELXT 2014/5 (Sheldrick, 2014)	
Refinement method	Full-matrix least-squares on F^2	
Refinement program	SHELXL-2018/3 (Sheldrick, 2018)	
Function minimized	$\Sigma\, w(F_o^2 - F_c^2)^2$	
Data / restraints / parameters	1260 / 18 / 89	
Goodness-of-fit on F^2	1.124	
Δ/σ_{max}	0.002	
Final R indices	1236 data; I>2σ(I)	R1 = 0.0225, wR2 = 0.0619

	all data	R1 = 0.0228, wR2 = 0.0621
Weighting scheme	$w=1/[\sigma^2(F_o^2)+(0.0311P)^2+16.1768P]$ where $P=(F_o^2+2F_c^2)/3$	
Largest diff. peak and hole	0.432 and -0.904 eÅ^{-3}	
R.M.S. deviation from mean	0.064 eÅ^{-3}	

Table S14. Bond lengths (Å) for Tris SbMnCl.

Mn1-Cl1#3	2.5848(5)	Mn1-Cl1#1	2.5849(5)
Mn1-Cl1#4	2.5849(4)	Mn1-Cl1#8	2.5850(4)
Mn1-Cl1#6	2.5850(4)	Mn1-Cl1	2.5851(5)
Sb1-Cl1#3	2.5848(5)	Sb1-Cl1#1	2.5849(5)
Sb1-Cl1#4	2.5849(4)	Sb1-Cl1#8	2.5850(4)
Sb1-Cl1#6	2.5850(4)	Sb1-Cl1	2.5851(5)
Mn2-Cl3	2.3832(6)	Mn2-Cl3#10	2.3833(6)
Mn2-Cl3#7	2.3833(6)	Mn2-Cl2#11	2.6378(8)
Mn2-Cl2	2.6380(7)	N1-C2#9	1.5100(17)
N1-C2#5	1.5100(18)	N1-C2	1.5101(17)
N1-H1	1.0	N2-C1	1.484(2)
N2-H2AA	0.83(3)	N2-H2BB	0.88(3)
N2-H2CC	0.87(3)	C1-C2	1.525(2)
C1-H1A	0.99	C1-H1B	0.99
C2-H2A	0.99	C2-H2B	0.99
O1-O2#9	1.086(12)	O1-O2#5	1.086(13)
O1-O2	1.086(12)	O2-O3#2	1.484(13)

Symmetry transformations used to generate equivalent atoms:

#1 -x+2/3, -y+4/3, -z+4/3
#2 -x+5/3, -y+1/3, -z+4/3
#3 y-1/3, -x+y+1/3, -z+4/3
#4 x-y+2/3, x+1/3, -z+4/3
#5 -y+1, x-y, z
#6 -y+1, x-y+1, z
#7 -y+2, x-y+1, z
#8 -x+y, -x+1, z
#9 -x+y+1, -x+1, z

#10 -x+y+1, -x+2, z
#11 x-y+1, -y+2, -z+3/2

Table S15. Bond angles (°) for Tris SbMnCl.

Cl1#3-Mn1-Cl1#1	89.616(15)	Cl1#3-Mn1-Cl1#4	89.615(15)
Cl1#1-Mn1-Cl1#4	89.615(15)	Cl1#3-Mn1-Cl1#8	90.388(14)
Cl1#1-Mn1-Cl1#8	90.388(14)	Cl1#4-Mn1-Cl1#8	179.996(18)
Cl1#3-Mn1-Cl1#6	180.0	Cl1#1-Mn1-Cl1#6	90.386(14)
Cl1#4-Mn1-Cl1#6	90.386(14)	Cl1#8-Mn1-Cl1#6	89.611(14)
Cl1#3-Mn1-Cl1	90.388(14)	Cl1#1-Mn1-Cl1	180.0
Cl1#4-Mn1-Cl1	90.388(14)	Cl1#8-Mn1-Cl1	89.609(14)
Cl1#6-Mn1-Cl1	89.610(14)	Cl1#3-Sb1-Cl1#1	89.616(15)
Cl1#3-Sb1-Cl1#4	89.615(15)	Cl1#1-Sb1-Cl1#4	89.615(15)
Cl1#3-Sb1-Cl1#8	90.388(14)	Cl1#1-Sb1-Cl1#8	90.388(14)
Cl1#4-Sb1-Cl1#8	179.996(18)	Cl1#3-Sb1-Cl1#6	180.0
Cl1#1-Sb1-Cl1#6	90.386(14)	Cl1#4-Sb1-Cl1#6	90.386(14)
Cl1#8-Sb1-Cl1#6	89.611(14)	Cl1#3-Sb1-Cl1	90.388(14)
Cl1#1-Sb1-Cl1	180.0	Cl1#4-Sb1-Cl1	90.388(14)
Cl1#8-Sb1-Cl1	89.609(14)	Cl1#6-Sb1-Cl1	89.610(14)
Cl3-Mn2-Cl3#10	120.0	Cl3-Mn2-Cl3#7	120.0000(10)
Cl3#10-Mn2-Cl3#7	120.0000(10)	Cl3-Mn2-Cl2#11	90.0
Cl3#10-Mn2-Cl2#11	90.0	Cl3#7-Mn2-Cl2#11	90.0
Cl3-Mn2-Cl2	90.0	Cl3#10-Mn2-Cl2	90.0
Cl3#7-Mn2-Cl2	90.0	Cl2#11-Mn2-Cl2	180.0
C2#9-N1-C2#5	110.46(10)	C2#9-N1-C2	110.45(10)
C2#5-N1-C2	110.45(10)	C2#9-N1-H1	108.5
C2#5-N1-H1	108.5	C2-N1-H1	108.5
C1-N2-H2AA	112.7(17)	C1-N2-H2BB	111.5(15)
H2AA-N2-H2BB	107.(2)	C1-N2-H2CC	107.6(15)
H2AA-N2-H2CC	109.(2)	H2BB-N2-H2CC	109.(2)
N2-C1-C2	109.33(13)	N2-C1-H1A	109.8
C2-C1-H1A	109.8	N2-C1-H1B	109.8
C2-C1-H1B	109.8	H1A-C1-H1B	108.3

N1-C2-C1	109.96(13)	N1-C2-H2A	109.7
C1-C2-H2A	109.7	N1-C2-H2B	109.7
C1-C2-H2B	109.7	H2A-C2-H2B	108.2
O2#9-O1-O2#5	118.1(4)	O2#9-O1-O2	118.1(4)
O2#5-O1-O2	118.1(4)	O1-O2-O3#2	140.2(10)

Symmetry transformations used to generate equivalent atoms:
#1 -x+2/3, -y+4/3, -z+4/3
#2 -x+5/3, -y+1/3, -z+4/3
#3 y-1/3, -x+y+1/3, -z+4/3
#4 x-y+2/3, x+1/3, -z+4/3
#5 -y+1, x-y, z
#6 -y+1, x-y+1, z
#7 -y+2, x-y+1, z
#8 -x+y, -x+1, z
#9 -x+y+1, -x+1, z
#10 -x+y+1, -x+2, z
#11 x-y+1, -y+2, -z+3/2

Table S16. Torsion angles (°) for Tris SbMnCl.

C2#3-N1-C2-C1	-156.36(14)	C2#2-N1-C2-C1	81.1(2)
N2-C1-C2-N1	-167.60(13)	O2#3-O1-O2-O3#1	144.0(6)
O2#2-O1-O2-O3#1	-9.(3)		

Symmetry transformations used to generate equivalent atoms:
#1 -x+5/3, -y+1/3, -z+4/3
#2 -y+1, x-y, z
#3 -x+y+1, -x+1, z

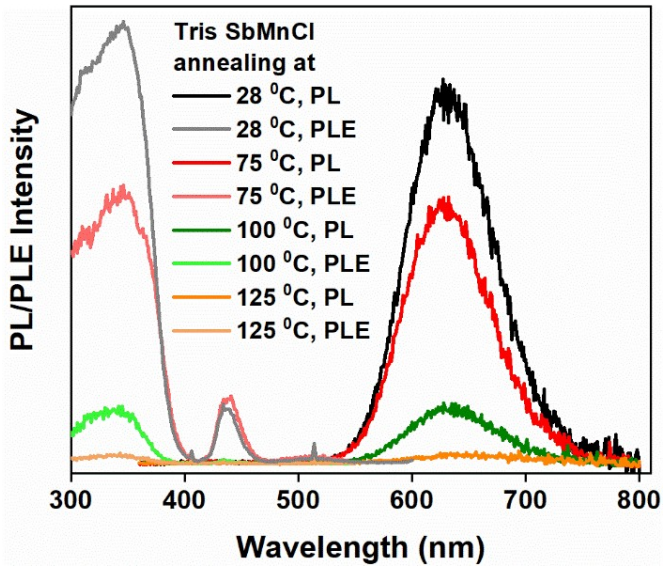

Figure S15: PL/PLE characterization of Tris SbMnCl hybrid annealed at different temperatures when excited at 340 nm.

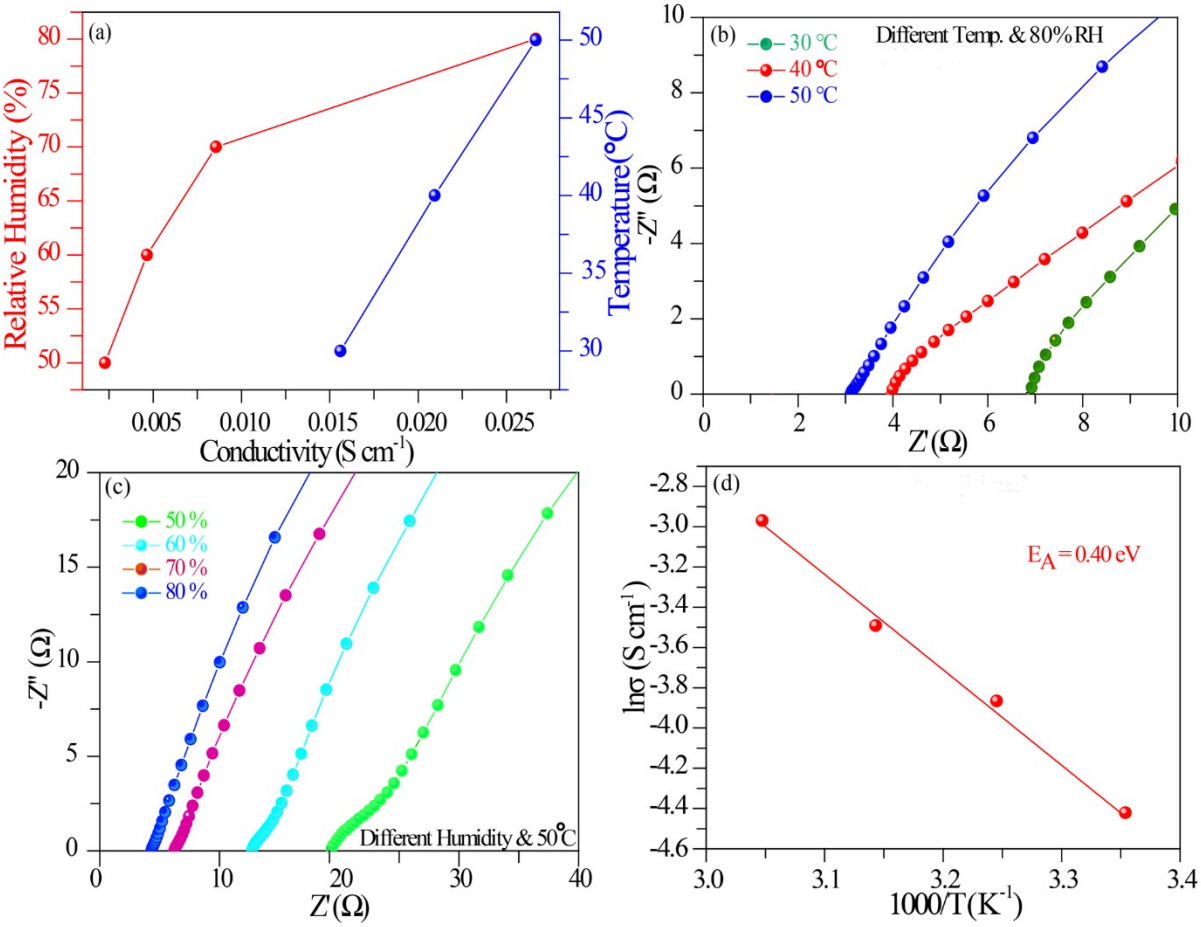

Figure S16: Electrochemical proton conductivity measurements of Tris SbMnCl hybrid as a function of a) temperature and relative humidity (RH); b) electrochemical impedance spectroscopy (EIS) measurements under 80% RH at different temperatures; c) EIS spectra measured at 50 °C with various RH; d) Arrhenius plots of conductivities of Tris SbMnCl hybrid at different temperatures.

Table S17: Comparison of proton conductivity of reported proton-conducting porous materials.

Sr. No	Compound Name	T (°C)	RH (%)	σ (S cm^{-1})	Reference
1	Nafion	80	98	~1 x10^{-1}	*J. Polym. Sci., Part B: Polym. Phys.*, **2011**, *49*, 1437.
2	PTSA@TpAzo COFM	80	95	7.8 x 10^{-2}	*Angew. Chem. Int. Ed.*, **2018**, *57*, 10894.
3	**Tris SbMnCl hybrid**	**50**	**80**	**5.6 x 10^{-2}**	**This work**
4	PCMOF-10	70	95	3.55 x 10^{-2}	*J. Am. Chem. Soc.*, **2015**, *137*, 7640.
5	Im@MOF-808	65	99	3.45 x 10^{-2}	*ACS Appl. Mater. Interfaces*., **2019**, *11*, 9164.
6	BIP	95	95	3.2 x 10^{-2}	*J. Am. Chem. Soc.*, **2019**, *141*, 14950.
7	PCMOF21/2	85	90	2.1 x 10^{-2}	*J. Am. Chem. Soc.*, **2013**, *135*, 963.
8	HOF-GS-11	30	95	1.8 x 10^{-2}	*Angew.Chem. Int. Ed.*, **2016**, *55*, 10667.
9	LiCl@RT-COF-1	40	100	6.45 x 10^{-3}	*J. Am. Chem. Soc.*, **2017**, *139*, 10079.
10	im@TPB-DMTP-COF	130	0	4.37 x 10^{-3}	*Nature. Mater.*, **2016**, 15, 722.
11	PCMOF-5	62	98	4.0 x 10-3	*J. Am. Chem. Soc.*, **2013**, *135*, 1193.
12	trz@TPB-DMTP-COF	130	0	1.1 x 10^{-3}	*Nature. Mater.*, **2016**, 15, 722.
13	PA@Tp-Azo	25	98	9.90 x 10^{-4}	*J. Am. Chem. Soc.*, **2014**, *136*, 6570.
14	PCF-1	30	95	2.03 x 10^{-4}	*J. Mater. Chem. A*, **2017**, *5*, 13659.
15	RT-COF-1AcB	40	100	1.07 × 10^{-4}	*J. Am. Chem. Soc.*, **2017**, *139*, 10079.

References

1. Phang, W. J.; Jo, H.; Lee, W. R.; Song, J. H.; Yoo, K.; Kim, B.; Hong, C. S., Superprotonic Conductivity of a UiO-66 Framework Functionalized with Sulfonic Acid Groups by Facile Postsynthetic Oxidation, Angew Chem. Int. Edn., **2015,** *54* (17), 5142-5146.